Available online at www.sciencedirect.com
SCIENCE DIRECT®
Ocean Engineering 31 (2004) 1683–1712
OCEAN ENGINEERING
www.elsevier.com/locate/oceaneng

An inverse hull design approach in minimizing the ship wave

Po-Fan Chen [a,b], Cheng-Hung Huang [c,*]

[a] *Department of Systems and Naval Mechatronic Engineering, National Cheng Kung University, Tainan, Taiwan, Republic of China*

[b] *Design Department, China Shipbuilding Corporation, Kaohsiung, Taiwan, Republic of China*

[c] *Department of Systems and Naval Mechatronic Engineering, National Cheng Kung University, Tainan, Taiwan, Republic of China*

Received 9 April 2003; accepted 1 August 2003

Abstract

The Levenberg–Marquardt Method (LMM) and a panel code for solving the wave-making problem are utilized in an inverse hull design problem for minimizing the wave of ships. A typical catamaran is selected as the example ship for the present study. The hull form of the catamaran is described by the B-spline surface method so that the shape of the hull can be completely specified using only a small number of parameters (i.e. control points). The technique of parameter estimation for the inverse design problem is thus chosen. The LMM of parameter estimation, which is the combination of steepest descent and Newton's methods, has been proven to be a powerful tool for the inverse shape design problem. For this reason it is adopted in the present study.

In the present studies, the inverse hull design method can not only be applied to estimate the hull form based on the known wave data of the target ship but can also be applied to estimate the unknown hull form based on the reduced wave height. The optimal hull forms of minimizing wave for a typical catamaran in deep water at service speed and at the critical speed of shallow water are estimated, respectively. Moreover, a new hull form with the combining feature of the optimal hull forms for deep water and shallow water is performing well under both conditions. The numerical simulation indicates that the hull form designed by inverse hull design method can reduce the ship wave significantly in comparison with the original hull form.

* Corresponding author. Tel.: +886-6-274-7018; fax: +886-6-274-7019.
E-mail address: chhuang@mail.ncku.edu.tw (C.-H. Huang).

0029-8018/$ - see front matter © 2004 Published by Elsevier Ltd.
doi:10.1016/j.oceaneng.2003.08.010

Nomenclature

B	position vector of the control points
N, **M**	B-spline basis function
Q	surface data points
q	magnitude of velocity
r	distance between source point and field point
U_o	magnitude of the uniform onset flow velocity
h	wave elevation
g	acceleration of gravity
V	displacement volume
H	target variables (wave heights and weighted displacement volume)
Fn_L	Froude number
Fn_d	depth Froude number
L	ship length
d	water depth
Cw	wave resistance coefficient
Cp	pressure coefficient

Greeks

Ψ	Jacobian matrix
Ω	computational domain
λ	damping parameter
ϕ	velocity potential
σ	source density
σ_h	deviation of wave elevation between the target wave and the estimated wave
ω	weight coefficient

Superscript

^	estimated value
n	iterative index
T	transport matrix

Keywords: Inverse design; Ship wave; Hull optimization; B-spline surface; Linearized free surface condition; Critical speed; Shallow water; Catamaran

1. Introduction

Recently, following the development of the modern high-speed ferry, worldwide attention has been attracted to the wash wave problem of these fast vessels. According to Wood (2000), the high-speed ferries generate two groups of wash

waves with periods of 3–5 s and 8–10 s. The long period waves are generally not easily visible from the ship due to their low amplitude. These long waves contain more energy than short waves and they also travel faster than short waves, so they will reach the beach or a small boat in open sea earlier than the short period visible wave. In addition to this dangerous phenomenon, the wash waves will also disturb marine life, damage the coast and relevant constructions. To reduce the risk of wash wave damage, the authorities may impose speed limitation on the fast ferries on some parts of their route. This leads to an increase in crossing time and operation cost.

The study of wash wave can be distinguished into several fields. Some focus on the behavior of wash wave approaching the coast as in Yang et al. (2001), the others focus on the developing of the optimal hull design to minimize wash wave as in Day and Doctors (2001) and Leer-Andersen and Larsson (1999). As one of the naval architects, this paper is devoted to the latter. To perform the hull form optimization design, it involves many issues such as the selection of proper objective function, optimal algorithm, geometric description of ship hull surface, reliable CFD program, design variable and constraints.

For the objective function of minimizing ship wave, the direct choices are the wave height along the ship's side, wave pattern and wave cut at some distance outside the vessel. These are examined in the present paper.

Yang et al. (2002) used four CFD methods to explore the minimization problem of the calm-water-drag of a trimaran. With regards to minimizing the wash waves of catamarans, Leer-Andersen and Larsson (1999) utilized the method of moving asymptotes (MMA) to perform the non-interactive optimization. The hull form optimization scheme of these studies was to search for the minimum value among a series of systematic varied hulls. For such kinds of hull form optimization algorithm, we classified it as the direct method. By contrast, the present inverse method, which predicts the hull form directly according to the desired ship wave, it is the most efficient way to optimise the hull form design with the minimum wash wave. In addition, since the literature about inverse hull design method is limited, it is worth introducing it to the ship designers and researchers.

The Levenberg-Marquardt Method (LMM) method has been shown to be a powerful algorithm in inverse calculations (Huang and Ozisik, 1991; Huang and Huang, 1994; Huang and Wang, 1996; Huang et al., 1998; Chen and Huang, 2002), especially in parameter estimations. The inverse design method had been applied to predict the hull form according to the desired hull pressure distribution by Huang et al. (1998). Sequentially it was applied to optimize the hull form based on the preferable wake distribution in the propeller disk plane by Chen and Huang (2002).

There are two major differences between Chen and Huang (2002) and this study. The first one is that the design target is changed from the axial wake at propeller plane to the ship wave and the constraint on displacement volume is also considered. The second one is that the direct problem (wave-making problem) can be solved with the potential theory and the panel code is utilized, however Chen and Huang (2002) solved the flow field with the RANS solver but the free surface is

excluded in the calculation due to the assumption of the zonal approach (Larsson et al., 1989).

The advantage of applying the inverse scheme is that the estimated hull is directly related to the given wave distribution. If a small wave is assigned, the predicted hull can be one of the optimal hulls with minimizing ship wave. If the wave height is too small or too unrealistic, the wave height of the inverse predicted hull is still the closest wave to the target value. However, unlike the hull pressure, distribution is directly located on the hull surface and, unlike the propeller wake, is behind the ship stern, the wave beside the ship is not so sensitive to the hull shape. For instance, the wave height may be identical for the minor change of hull form. Therefore, how to establish the certain correlation is one of the challenges in this paper. To improve the accuracy of the inverse hull prediction, the constraint on displacement volume is, for the first time, introduced into the LMM method. According to our study, it indeed improves the quality of inverse hull prediction so should be considered as the contribution of this study.

For the numerical representation of complex hull surface used in optimization design methods, various methods can be found in the literature, for instance, Lin et al. (1963); Wyatt and Chang (1990); Larsson et al. (1992); Leer-Andersen and Larsson (1999); Lowe et al. (1994), and Huang et al. (1998). Due to the simplicity of the method, the B-spline surface technique was adopted by Chen and Huang (2002) to manipulate the hull form in the inverse hull design problem. By the same token, it is selected in the present study.

The desirable CFD tools for hull form optimization of minimizing wave should have the ability of covering the limited range of ship speed, performing the shallow water calculation, good accuracy but not too time consuming, easy to converge, and can be submitted into subroutine for non-interactive calculation. Chen and Huang (2002) had deduced an inverse algorithm that communicates with the SHIPFLOW (Larsson, 1999) code through data transportation and thus establishes an inverse design problem for hull surface. After modifying the program, the inverse algorithm of LMM utilizing SHIPFLOW code as the subroutine is used for solving the minimizing ship wave problem.

The important constraints for the minimization of wave of the modern high-speed ferry are the displacement, deck area, transom stern, and calm water resistance. According to Leer-Andersen and Larsson (1999), the wave resistance can be reduced in the case of the minimum wash wave design, so it is excluded from the constraints of the present study. This presumption has been confirmed by the case studies in the following section. According to our study, the estimated results would be improved if the transom stern is allowed to be moved by the geometry control points in the optimization process but this does not reduce the area for the arrangement of propulsion device. Therefore, the necessary constraints left are the displacement and deck area.

To design the ship with minimizing wave, the target wave can be set as a smaller value from the existing parent ship. The inverse method can predict the corresponding hull form of such a small wave. If the wave height is too small or too

unrealistic, the wave height of the inverse predicted hull is still the closest wave to the target value.

The method of hull surface generation and B-spline surface fitting is described in Section 2. The method used to calculate the wave distribution around the advancing ship, i.e. the direct problem is introduced in Section 3. The inverse design problem involving the definition of cost function and Levenberg–Marquardt algorithm is addressed in Section 4. The computational procedure is summarized in Section 5. Finally, a systematic study on a catamaran is detailed in Section 6.

2. Hull generation and B-spline surface fitting

To manipulate the hull surface with a small number of parameters (i.e. control points), the B-spline surface method is introduced to describe the hull form. It is adopted from the Huang et al. (1998) paper.

2.1. Hull generation

Consider a Cartesian product parametric B-spline surface given by

$$Q(u,w)=\sum_{i=1}^{n+1}\sum_{j=1}^{m+1}B_{i,j}N_{i,k}(u)M_{j,l}(w)\quad 2\le k\le n+1;2\le l\le m+1 \tag{1}$$

where

$$N_{i,1}=\begin{cases}1 & \text{if } x_i\le u<x_{i+1}\\ 0 & \text{otherwise}\end{cases}$$

$$N_{i,k}(u)=\frac{(u-x_i)N_{i,k-1}(u)}{x_{i+k-1}-x_i}+\frac{(x_{i+k}-u)N_{i+1,k-1}(u)}{x_{i+k}-x_{i+1}} \tag{2a}$$

and

$$M_{j,1}=\begin{cases}1 & \text{if } y_j\le w<y_{j+1}\\ 0 & \text{otherwise}\end{cases}$$

$$M_{j,l}(w)=\frac{(w-y_j)M_{j,l-1}(w)}{y_{j+l-1}-y_j}+\frac{(y_{j+l}-w)M_{j+1,l-1}(w)}{y_{j+l}-y_{j+1}} \tag{2b}$$

where x_i , y_j are the elements of a uniform knot vector, k and l are the order of the B-spline surface in the u and w directions, and n and m are one less than the number of polygon net points in the u and w directions, respectively. Here $Q(u,w)$ are the surface data points. The N and M basis functions can be determined from the knot vector and the parameter values u and w. $B_{i,j}$ are the required polygon net points (control points). If $B_{i,j}$ are given, the surface data points $Q(u,w)$ can be calculated from Eq. (1).

2.2. B-spline surface fitting

When the surface is described by external data, it is convenient to obtain an initial non-flat B-spline surface approximating the hull for subsequent real time interactive modification. This requires determining the defining polygonal net from an existing network of three-dimensional surface data points.

For each known surface data point, Eq. (1) provides a linear equation in the unknown $B_{i,j}$'s and similarly for all the surface data points. In matrix notation this can be written as

$$[Q] = [C][B] \tag{3}$$

Since for any arbitrary $r \times s$ topologically rectangular surface point data, $[C]$ is not normally square, a solution can be obtained only in some mean sense. In particular

$$[B] = [[C]^T[C]]^{-1}[C]^T[Q] \tag{4}$$

The u and w parametric values for each surface data are obtained using a chord length approximation. For detailed discussions, please refer to Huang et al. (1998).

3. Direct problem

The direct problem is to calculate the wave distribution around the advancing ship. The potential method briefly introduced in the following is appropriate for solving this problem.

A steady and irrotational flow is considered here with inviscid and incompressible fluid properties. A right-handed coordinate system XYZ is employed with the origin on the mean free surface, x positive in the direction of the uniform flow, and z positive upwards. The ship piercing the free surface is assumed to be in a uniform onset flow of velocity U_o. The flow field around the ship may be described by a velocity potential ϕ, which is generated by distribution of sources on the hull surface S and by the uniform onset flow in the x direction.

$$\phi = \oint_S \frac{\sigma(q)}{r(p,q)} ds + U_o x \tag{5}$$

where $\sigma(\mathrm{q})$ is the source density on the surface element ds and $r(p,q)$ is the distance from the point q to the field point p where the potential is being evaluated.

The potential ϕ in Eq. (5) is governed by the Laplace equation

$$\nabla^2\phi = 0 \tag{6}$$

On the wetted hull surface the solid boundary condition is

$$\frac{\partial\phi}{\partial n} = \phi_n = 0 \tag{7}$$

where n denotes the outward normal. At infinity, the disturbance due to the body

must vanish, i.e.

$$\nabla\phi \to (U_o, 0, 0) \quad \text{as} \quad r \to \infty \tag{8}$$

At the free surface, two boundary conditions must be imposed. The first one is that the flow must be tangent to the surface, i.e. the kinematics boundary condition

$$\phi_X h_X + \phi_Y h_Y - \phi_Z = 0 \tag{9}$$

here, h is the wave elevation, i.e. $h = z(x, y)$.

The second one is that the pressure must keep constant and this is the dynamic boundary condition

$$gh + \frac{1}{2}(\nabla\phi \cdot \nabla\phi - U_0^2) = 0 \tag{10}$$

Further, no upstream wave must be generated. Since Eqs. (9) and (10) are nonlinear and are to be satisfied on the unknown wavy surface $z = h(x, y)$. The perturbation method is introduced to yield the linearized free surface boundary condition. A double model is used as the first basic model solution for the free surface computation, although the numerical results with linearized free surface condition are less accurate than those with the nonlinear free surface condition. However, there are two inherent disadvantages for applying the nonlinear free surface solution in the optimization process: The first one is time-consuming (normally requiring about 5–10 iterations), the second one is that it may meet the divergent problem especially in the critical speed case of shallow water. In the divergent case the wave will have substantial oscillation so that it is an obstacle for construction of the Jacobian matrix in the inverse design approach. Therefore, the linear free surface solution is used in the inverse design process. To confirm the consistency, the nonlinear solution is applied for the deep-water condition to check the final optimal hull.

For the calculation of shallow water conditions, a non-permeable surface at the sea bottom is enforced. Instead of distributing the panels on the sea bottom, a symmetry condition is used at the position of the sea bottom, i.e. there is a mirror image of the hull and the free surface about this plane. The flow is not computed at the symmetry plane, so it is less time consuming than computing the flow at the panels on the sea bottom.

A typical catamaran quoted from SHIPFLOW's example bank is selected as the initial ship, i.e. parent ship for the present study. The example of the penalization for hull and the free surface is illustrated in Fig. 1. Due to the symmetry of the catamaran, only the left part of the flow domain is calculated so that the computing time can be saved. The panel number used in all runs is 360 for the left hull and 960 for the left domain of free surface.

4. Inverse hull design problem

For the inverse hull design problem, the main hull is regarded as being unknown and is dominated by a set of control points. In addition, the desired distributions

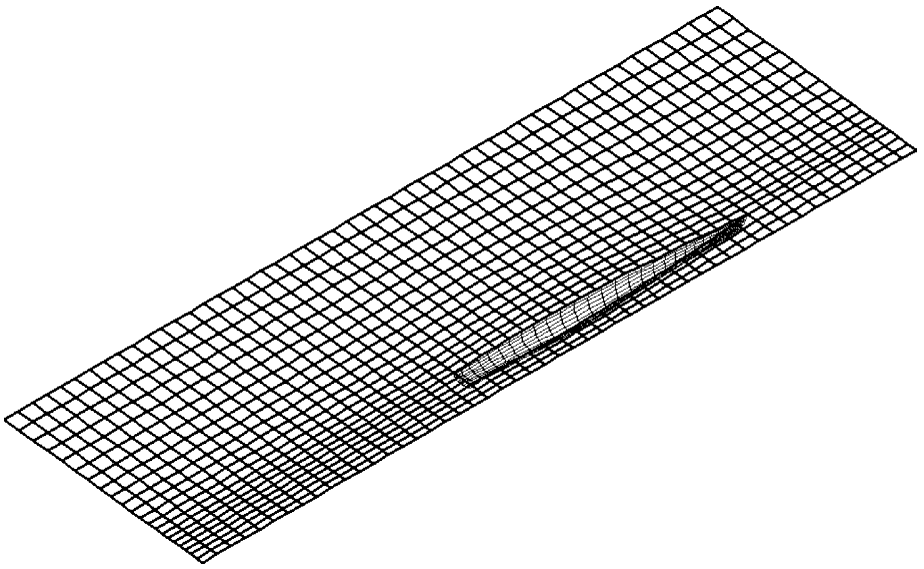

Fig. 1. Penalization example for hull and free surface.

of dimensionless wave height, h_i, on the free surface and desired displacement volume, V, are considered available. Let the desired wave height be denoted by h_i, $i = 1$ to I, where I represents the number of wave data, the inverse design problem can be stated as follows: By utilizing the above-mentioned desired wave height h_i and volume V, design the new hull. To minimize the outgoing wave, the inverse design is focused on the outside part of main hull, i.e. the portside of the left hull in our present study.

The solution of the present inverse design problem is obtained in such a way that the following function is minimized

$$\mathrm{f}[\hat{\mathbf{\Omega}}(\hat{\mathbf{B}})] = \sum_{i=1}^{I} [\hat{\mathrm{h}}_i(\hat{\mathbf{B}}_j) - \mathrm{h}_i]^2 + \omega[\hat{\mathbf{V}}(\hat{\mathbf{B}}_j) - \mathrm{V}]^2 \; ; \quad \mathrm{j} = 1 \text{ to } \mathrm{J} \tag{11a}$$

Here, $\hat{\mathbf{h}}_i$ are the estimated or computed wave heights along shipside. Here the hat "^" denotes the estimated quantities, V is the target displacement volume and $\hat{\mathbf{V}}(\hat{\mathbf{B}}_j)$ is the estimated or computed displacement volume, ω is a Lagrangian multiplier for the equality constraint on volume while the error on the target wave heights is to be minimized. The proposed Lagrangian approach will improve the results in the inverse design process. The wave height h and displacement volume V in the above equation are nondimensional by the ship length and by the target displacement volume, respectively. These quantities are determined from the solution of the direct problem given previously by using an estimated hull form $\hat{\mathbf{\Omega}}(\hat{\mathbf{B}})$. J represents the number of control points. In the present study three boundaries of

hull (i.e. keel, stem profile and deck area) are fixed, only the transom is movable. Thus the movable control points are $J = (n) \times (m-1)$.

The previous studies of inverse hull design problems presented by Huang et al. (1998) and Chen and Huang (2002) did not pay attention to maintaining the displacement volume. However, the displacement is an important factor to the hull form design of the modern high-speed ferry. Thus the constraint of displacement volume is considered in the above cost function.

To simplify Eq. (11a), the variable of wave height and weighted displacement volume can be combined into one compact vector $\mathbf{H}$, $\mathbf{H} = H_i = \{h_1, h_2, \ldots.., h_I, \omega V\}$, and then Eq. (8) can be rewritten as follows:

$$f[\hat{\boldsymbol{\Omega}}(\hat{\mathbf{B}})] = \sum_{i=1}^{I+1}[\hat{\mathbf{H}}_i(\hat{\mathbf{B}}_j) - \mathrm{H}_i]^2 = \mathbf{G}^T\mathbf{G}\ ; \quad j = 1 \text{ to } J \tag{11b}$$

4.1. Levenberg–Marquardt method for minimization

If the wave height is measured at I points and the redesigned hull form is governed by J control points, Eq. (11) is minimized with respect to the estimated parameters Bj to obtain

$$\frac{\partial f[\hat{\boldsymbol{\Omega}}(\hat{\boldsymbol{B}})]}{\partial \hat{\boldsymbol{B}}} = \sum_{i=1}^{I+1}\left[\frac{\partial \hat{\boldsymbol{H}}_i(\hat{\boldsymbol{B}}_j)}{\partial \hat{\boldsymbol{B}}_j}\right]\left[\hat{\boldsymbol{H}}_i - \boldsymbol{H}_i\right] = 0;\ j = 1 \text{ to } J \tag{12}$$

where I should be equal to or greater than J; otherwise an underdetermined system of equations will be obtained and it is impossible to calculate the inverse solutions in this situation.

If the weight function is set to zero, i.e. $\omega = 0$, Eq. (12) is valid for the optimum wave study without displacement constraint. Eq. (12) is linearized by expanding $\hat{\mathbf{H}}_i(\hat{\mathbf{B}})$ in Taylor series and retaining the first order terms. Then a damping parameter λ^n is added to the resulting expression to improve convergence, leading to the Levenberg–Marquardt method (Marquardt, 1963) given by

$$(\mathbf{F} + \lambda^n\mathbf{I})\Delta\mathbf{B} = \mathbf{D} \tag{13a}$$

where

$$\mathbf{F} = \Psi^T\Psi \tag{13b}$$

$$\mathbf{D} = \Psi^T\mathbf{G} \tag{13c}$$

$$\Delta\mathbf{B} = \mathbf{B}^{n+1} - \mathbf{B}^n \tag{13d}$$

here the superscript n and T represent the iteration index and the transpose of matrix, respectively, $\mathbf{I}$ is the identity matrix, and Ψ denotes the Jacobian matrix defined as

$$\Psi \equiv \frac{\partial \mathbf{H}}{\partial \mathbf{B}^T} \tag{14}$$

The Jacobian matrix defined by Eq. (14) is determined by perturbing each unknown parameter B_j at one time and computing the resulting change in wave height from the solution of the direct problem, Eq. (6).

Eq. (13a) is now written in a form suitable for iterative calculation as

$$\mathbf{B}^{n+1} = \mathbf{B}^n + (\mathbf{\Psi}^T\mathbf{\Psi} + \lambda^n\mathbf{I})^{-1}\mathbf{\Psi}^T(\hat{\mathbf{H}} - \mathbf{H}) \tag{15}$$

The algorithm of choosing this damping value λ^n is described in detail in Marquardt (1963), so it is not repeated here.

5. Computational procedure

The iterative computational procedure for the present inverse design problem can be summarized as follows:

Choose the initial guess for control points **B** (obtained by using original hull form and B-spline surface fitting) at iteration 1 to start the computation.

Step 1. Solve the direct problem to obtain the estimated (or computed) wave height $\hat{\mathbf{h}}$ and displacement volume $\hat{\mathbf{V}}$.
Step 2. Construct the Jacobian matrix in accordance with Eq. (14).
Step 3. Update **B** from Eq. (15).
Step 4. Check the stopping criterion; if not satisfied, then go to Step 1 and iterate. The stopping criterion is defined as follows:

$$\mathrm{f}[\hat{\mathbf{\Omega}}(\hat{\mathbf{B}})] = \sum_{i=1}^{I+1}[\hat{\mathrm{H}}_i(\hat{\mathrm{B}}_j) - \mathrm{H}_i]^2 \leq \varepsilon \tag{16}$$

Due to the fact that the target function h_i is located neither on the hull surface nor in the downstream, the correlation between target function and control points is not very sensitive. If the given target wave height is out of reality, such as too small or unreasonable distribution, at first trial it is better to select slight loosing stopping criteria such as $\varepsilon = 6.0 \times 10^{-5}$.

6. Results and discussions

A conventional catamaran quoted from SHIPFLOW's example bank is used as the initial design for the entire study. This catamaran is identical to that used in Leer-Andersen and Larsson's paper (1999). The ship is 80 m in length and the service speed in deep water is set as 35 knots (i.e. the Froude number $\mathrm{Fn_L} = U_0/\sqrt{gL}$ is 0.6428). For the shallow water navigation, the depth Froude number $\mathrm{Fn}_d = U_0/\sqrt{gd}$ is used. The water depth is set as 10 m and the corresponding ship speed is 19.25 knots to yield the critical condition, i.e. $\mathrm{Fn}_d = 1$.

The hull form of the high-speed catamaran is of a streamline shape with simple geometry so that a lesser number of control points are required. After performing the study of surface fitting, the catamaran can be fitted well with 8×5 control

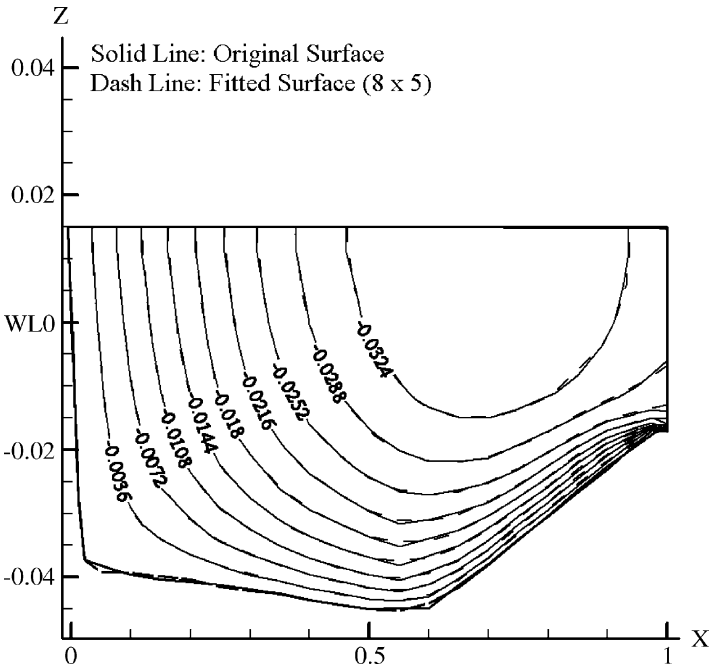

Fig. 2. Buttock plan for the original hull and the fitted surface using 8×5 control points.

points, which is illustrated in Fig. 2. Therefore, the number of the unknown control points B_j is chosen as 8×5 for the rest of this paper. To provide enough description of hull surface, we use 24×13 surface data points in u (ship's longitudinal direction) and v direction (ship's depth direction), respectively.

In order to show the validity of our inverse hull design algorithm in estimating the optimal hull form with the minimized wave, a series of studies are performed step by step in the following.

1. Select the proper objective function: The objective function is the wave profile data and the wave cut data. The wave profile data is obtained form the wave height data on the first strip of panels along the shipside. The wave height data for the wave cut method is obtained form the interpolation of the free surface panels at the specified distance outside the catamaran.
2. To explore the influence of displacement weight coefficient ω on the critical condition of shallow water, the optimal designs of hull forms with minimized wash wave are surveyed by using three different weight coefficients.
3. To find the optimal design of minimized wash wave in deep-water condition, two target wave heights were tested.
4. Averaging the control points of optimal hulls for deep water and shallow water generates a new hull form with the combining feature of both optimal

hull forms. Fortunately, the numerical simulation shows that the waves in both conditions are reduced significantly when comparing with the initial catamaran.

6.1. Numerical verification of the inverse hull design algorithm

To perform the fundamental calculation of the inverse hull design problem, a hull form with reduced waterplane area (hereafter simplified as semi-swath hull) is used as the target hull. This semi-swath hull is generated from the conventional catamaran by moving some control points along the water line 50% inward into the ship center. Both initial and target hull forms are shown in Figs. 3 and 4(a). The wave height data obtained from the solution of the direct problem, Eq. (6), are used as the objective wave height in the inverse problem. The conventional catamaran is used as the initial hull form. Apply the Levenberg–Marquardt method to perform the inverse design approach until the specified stopping criterion is satisfied. The estimated hull form is thus obtained. By comparing the body plan of the estimated hull form with the target hull form such as that illustrated in Figs. 4(b)–(d), and 6, we can judge if the inverse design is successful.

6.1.1. Study of the displacement constraint

The first step of this numerical investigation is to realize the difference between applying ($\omega \neq 0$) and not applying ($\omega = 0$) the volume constraint in the inverse hull design process. The wave profile data of semi-swath hull is used as the design

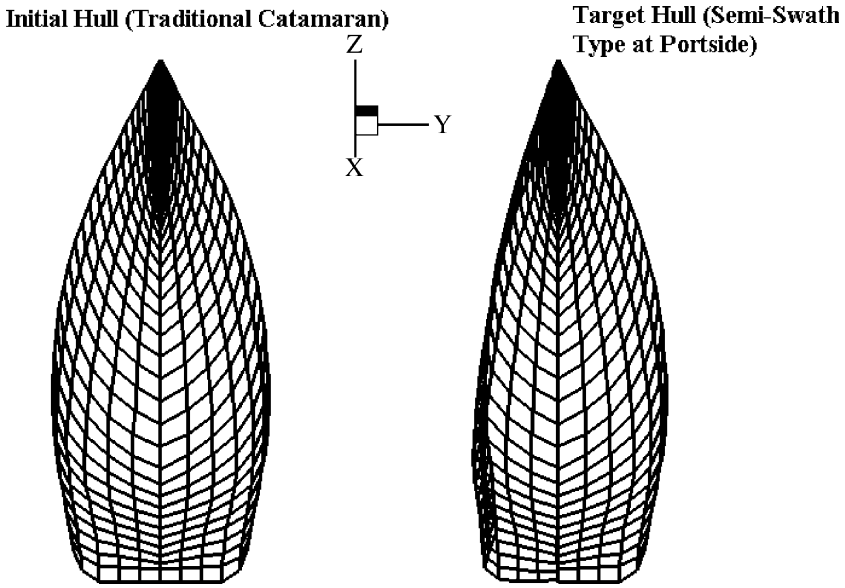

Fig. 3. Panelized hull for Initial and target hulls used in Section 6.1.

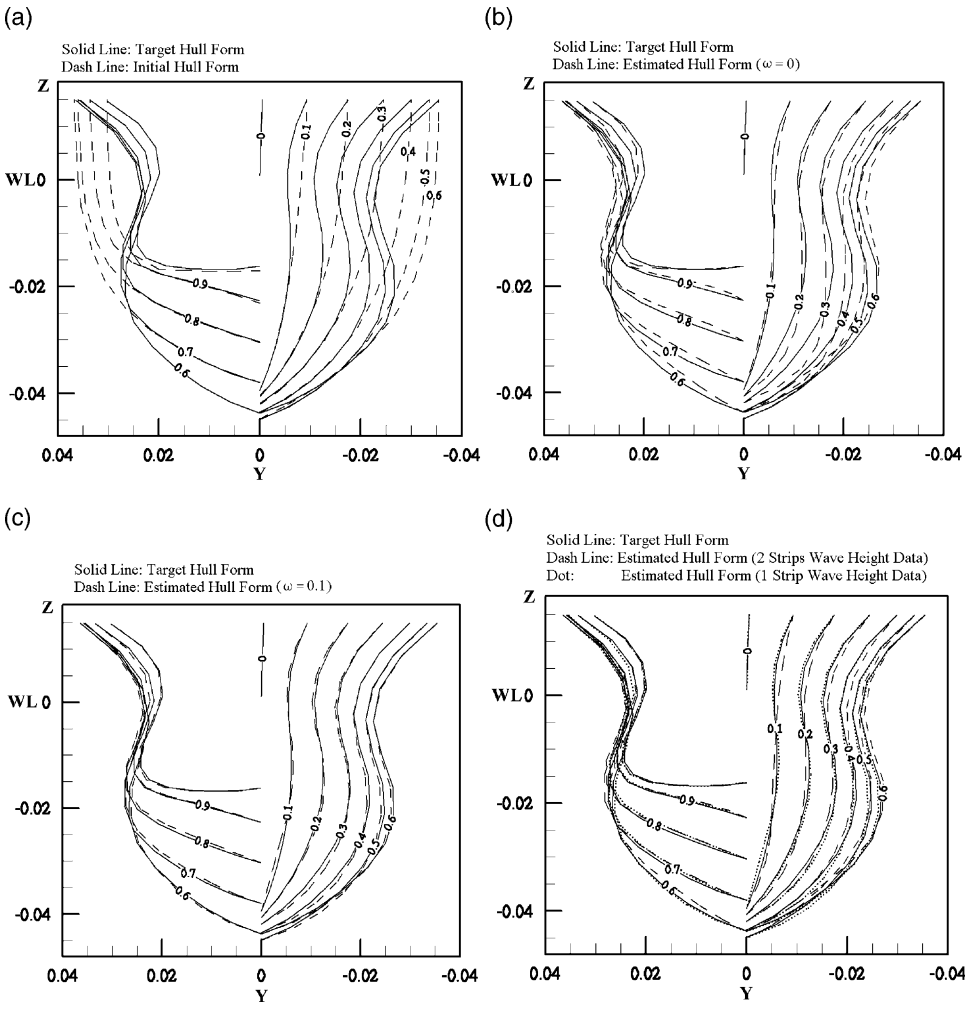

Fig. 4. Body plans for (a) the Initial hull and target hull (b) estimated hulls $\omega = 0$ (c) estimated hull $\omega = 0.1$ and (d) estimated hull by 2 strips wave data.

object and the present case is performed at deep water condition with the ship speed of 35 knots, i.e. $Fn_L = 0.6428$.

By setting the stopping criteria $\varepsilon = 1.0 \times 10^{-7}$ and following the Levenberg–Marquardt algorithm, a very accurate solution can be obtained for $\omega = 0$ and $\omega = 0.1$ with only six and seven iterations, respectively. The required CPU for $\omega = 0$ and $\omega = 0.1$ examples is approximately 9431 and 10,692 s on an SGI Octane machine, respectively. The deviations of wave height, σ_h, between estimated hull and target hull are only 2.78×10^{-8} and 1.48×10^{-8} for $\omega = 0$ and $\omega = 0.1$,

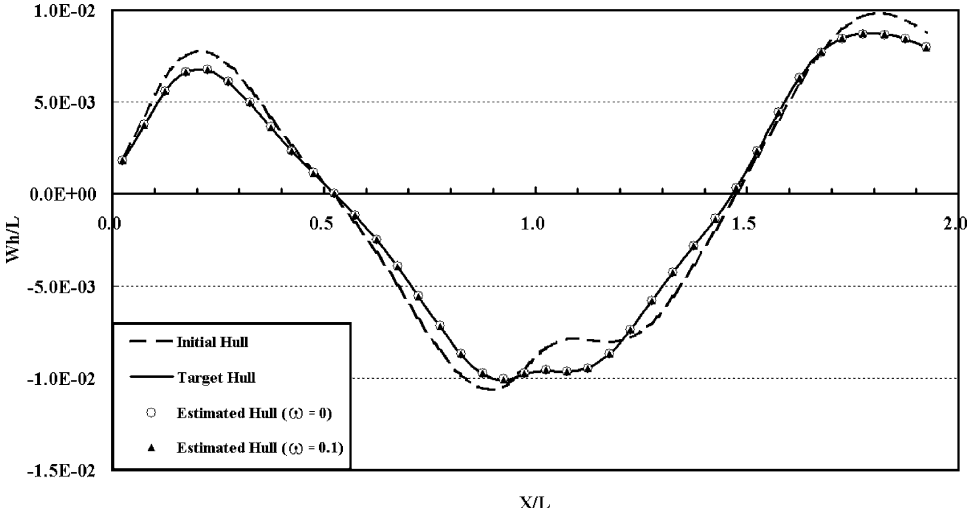

Fig. 5. Comparison of wave profile along catamaran's outside for the initial, target, and estimated hulls for $\omega = 0$ and 0.1.

respectively. Where σ_h is defined as follows

$$\sigma_{\mathrm{h}} = \sum_{i=1}^{I} \left| \hat{\mathrm{h}}_i - \mathrm{h}_i \right|^2 \tag{17}$$

here, $I = 39$ in the present example. Further information is detailed in Table 1. From Table 1, one can see that the wave resistance coefficient Cw and displacement volume of both estimated hulls is quite close to the target value. When the constraint for volume is applied, the displacement volume of the optimal hull is identical to that for the target hull.

The comparison of body plans for the initial, target and estimated hulls is illustrated in Fig. 4. From Fig. 4, we find that the estimated hull is very close to the target hull, therefore we concluded that the Levenberg–Marquardt method has been applied successfully in the present semi-swath case.

In addition to the above, a comparison of wave profile for the initial, target and two estimated hulls are shown in Fig. 5. In this figure, the coincidence of wave profiles between the target and the estimated hull are very good. Therefore, even the hull form is small deviated from the target ship, the wave profile will be almost the same. This non-sensitive phenomenon is the challenge of the presented study. By the aid of Lagrangian multiplier to the displacement constraint, the quality of the estimated hull form could be further improved.

6.1.2. Study of the design object—wave profile

The second step of this numerical investigation is to find out the proper objective function suitable for the inverse design method. For the above cases, the wave

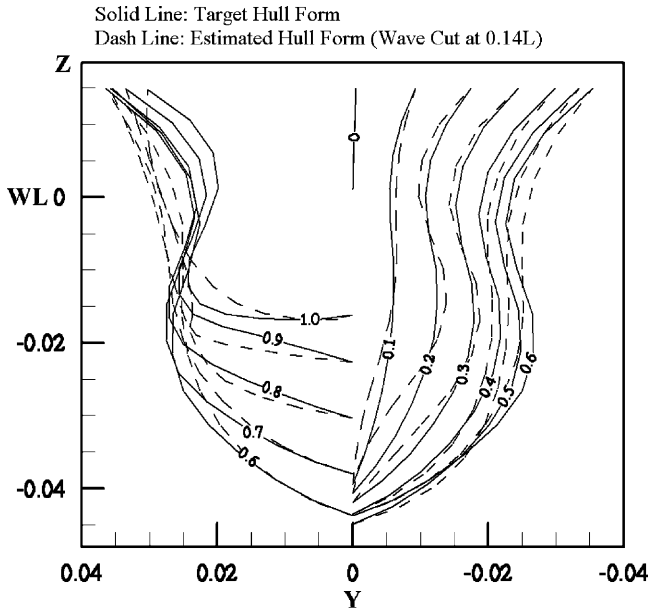

Fig. 6. Body plans for the target and estimated hulls using wave cut data as objective function.

profile data is used as the design object. This wave profile data is obtained from the panel center of the first strip contacting the ship's portside. To obtain the over-determined system of equations for the inverse solution, the number of wave height data I should be equal to or greater than the number of movable control points J. Will the solution converge faster or the predicted results become more accurate if more wave height data is utilized? To answer this, the wave height data next to the first strip of panels are also used as the design object.

For the design object of two strips of wave height, the stopping criteria is set as $\varepsilon = 1.0 \times 10^{-7}$ and the displacement constraint $\omega = 0.1$ is imposed. The initial hull is the same as the previous one. Following the LMM algorithm, a design solution

Table 1
The numerical results of inverse hull design in Section 6.1

Semi-swath (target ship)		$\omega = 0.0$ (used wave profile data)	$\omega = 0.1$ (used wave profile data)	$\omega = 0.1$ (used 2 strips wave height data)	$\omega = 0.1$ (used wave cut data at 0.14 L)
Cw_linear	100.00%	99.96%	99.85%	99.92%	98.500%
Volume	100.00%	100.51%	100.00%	100.08%	100.04%
σ_h	–	2.78E-08	1.48E-08	1.73E-08	1.06E-07
CPU (s)	65	9,431	10,692	9,148	9,164
Iteration	–	6	7	6	6

can be obtained with only six iterations, which is one iteration saved than the case using one strip of wave height data. The required CPU on an SGI Octane machine for this case is approximately 9148 s, which is approximately 1544 s saved than the case using one strip of wave height. The deviation of wave height, σ_h, between the estimated and target hulls is only 1.73×10^{-8}. The comparisons of body plans for the target and estimated hulls with one and two strips of wave height are also shown in Fig. 4(d). From Fig. 4(d), we note that the hull form estimated by two strips of wave data is also very close to the target hull but slightly worse than that for one strip case. The quality of inverse hull design for two strip wave height case can be improved by setting the stopping criteria ε more tight such as 1.0×10^{-8}, but this will increase at least one more iteration number and this will lose the advantage of using two strip wave data. In addition, the actual correlation of wave height between the first and second wave strips is undetermined so that it is impractical to give two strips of wave data as the design target in minimum wash wave. Therefore, it is not adopted for the study of the optimal hull in deep water and shallow water.

6.1.3. Study of the design object—wave cut

In addition to using the wave profile data as the design object, another design object is proposed by using the wave data at some fixed distance beside the ship, i.e. herein named as the wave cut. These data are interpolated from the free surface panels at the given distance.

The construction of sensitive matrix, i.e. Jacobian matrix, is very important to the LMM algorithm. The Jacobian matrix connects the change of wave cut data to the corresponding movement of hull form. Thus, if the wave cut location is too far away from the ship side, the selected wave cut data may be identical for various shape of the hull forms including a highly distorted hull form, and that may lead the direction problem solver SHIPFLOW to crash.

In order to prevent this unwanted situation, we placed the wave cut closer to the shipside or increased wave cut range in the longitudinal direction. For the later, it will largely increase the free surface panel in the downstream field and it will also increase the computational time in minimizing the ship wave. For this reason we choose to place the wave cut closer to the shipside. Considering that the center of the left hull is 0.095 L off the center plane of the catamaran and the outer point of the initial hull is located at around 0.1263 L, we place the wave cut at 0.14 L off the catamaran center.

After performing the inverse design calculation, we find that the estimated hull form based on wave cut data is less sensitive than that by wave profile data, therefore the stopping criteria should be slightly loosed to the value $\varepsilon = 2.0 \times 10^{-7}$. An estimated hull form is obtained after six iterations and the required CPU on an SGI Octane machine is approximately 9164 s. The wave height deviation is 1.06×10^{-7} which is almost one order higher than that for wave profile data. A comparison of body plans for the target and estimated hulls based on wave cut data is shown in Fig. 6 and the comparison of wave cut for the target and estimated hulls is plotted in Fig. 7. It is noted that the estimated hull form is deviated

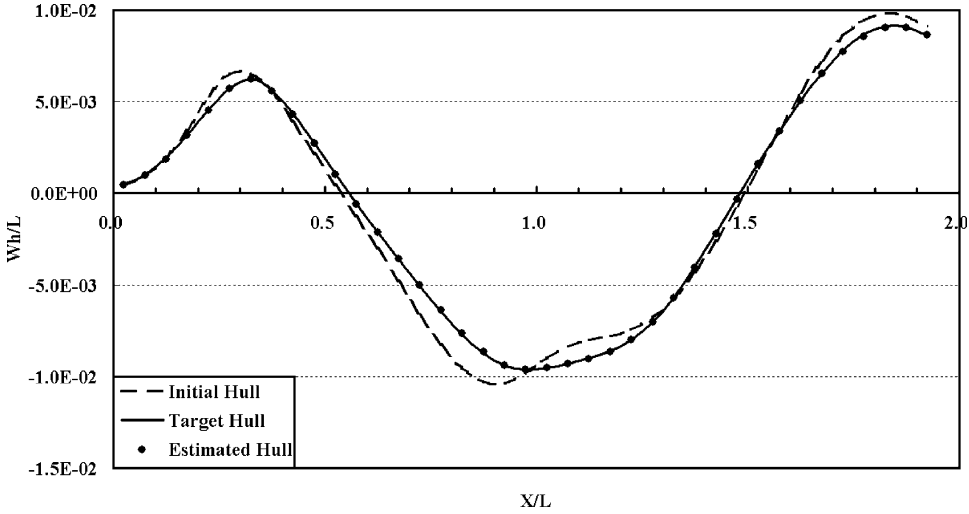

Fig. 7. Comparison of wave cut at 0.14 L off center plane for the initial, target, and estimated hulls using the wave cut data as the inverse design object.

from the target hull form even though the wave cut of both hulls is quite coincidental. Apparently, the correlation between the hull form and the wave cut length used in the present study is not good enough.

However, although the more long distance of wave cut in the downstream will improve the accuracy and obtain the convergent solution for the inverse prediction at traditional wave cut location such as 0.2 L, it requires distributing more panels on the outstretched free surface. Regarding that the CPU will be increased in the square order with the panel number, so it is less economic when comparing with using the wave profile data. In addition, it is more difficult to prepare more wave data for the optimal hull estimation of reduced ship wave if the wavelength number of wave cut is increased.

Therefore, we decide to utilize the wave profile data together with the Lagrangian multiplier to the displacement volume as the design target for the inverse design approach to estimate the optimal hull form of reduced ship wave in the following section.

6.2. *Minimizing wash wave in shallow water*

Three speed ranges can be classified for ships navigating in shallow water, they are subcritical ($Fn_d < 1$), critical ($Fn_d = 1$) and supercritical ($Fn_d > 1$) speeds, respectively. At the critical speed the wave crest becomes perpendicular to the ship track. Energy is continually pumped into the wave and the crest travels forward and outward at a speed equal to $\sqrt{gd}$. To illustrate how to minimize the wash wave by the inverse method, the catamaran is optimized at critical speed in the following studies.

The first step is to design the desired wave height. It is unnatural to pursue no wave in the 3-D flow domain. Regarding that the bow wave is in a high-pressure zone generated due to the stagnation point of stem, it makes no sense to define the target wave with a very small bow wave. Based on this recognition, we design the target wave height with 0.875 times of the bow wave of the initial hull form, i.e. the conventional catamaran. For the following wave trough at mid-ship region and the downstream wave, there should be some more improving space so we presume a factor of 0.6 times wave height of the initial hull. Such distribution features of the proposed target wave is reasonable for the minimizing ship wave and it is the same tendency as the optimal results of Leer–Andersen and Larsson's paper (1999). The wave profiles for the initial and target waves are plotted in Fig. 8.

The target displacement is set the same as the initial hull. Unlike the inverse hull estimation in the previous section, there may not exist such a real hull form that can perfectly match with such a target wave profile and the displacement value. Therefore, the estimated hull is the best approach to target value with the least square error.

To fine tune the Lagrangian multiplier for the equality constraint on volume, three values 0.01, 0.05 and 0.1 are studied. For the first value $\omega = 0.01$, it means the displacement are in the same order to one of the wave height data. There are 39 points of wave height data, so the influence of the displacement is only one fortieth of the target function. The bigger value $\omega = 0.1$ implies that the demand on the equality of volume is severer in the objective function.

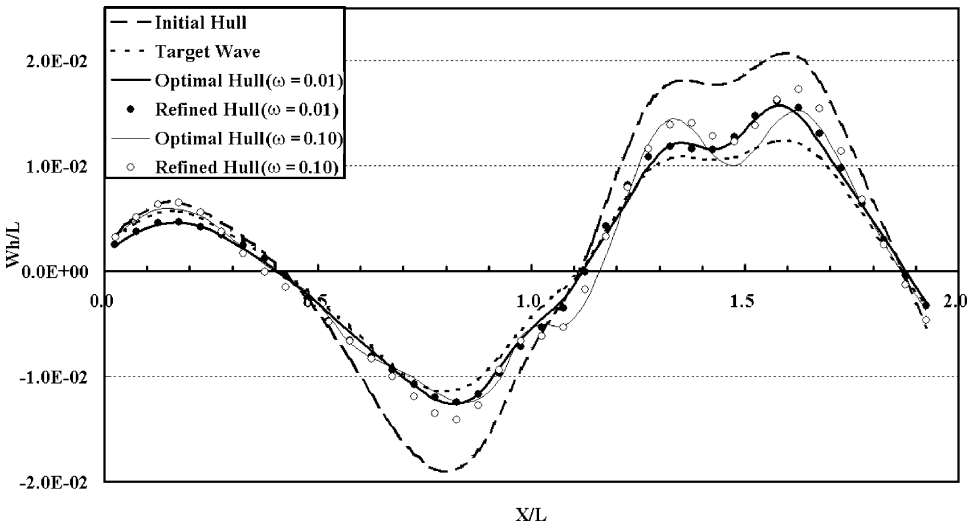

Fig. 8. Comparison of wave profile for the initial, target, optimal, and refined hulls with $\omega = 0.01$ and 0.10.

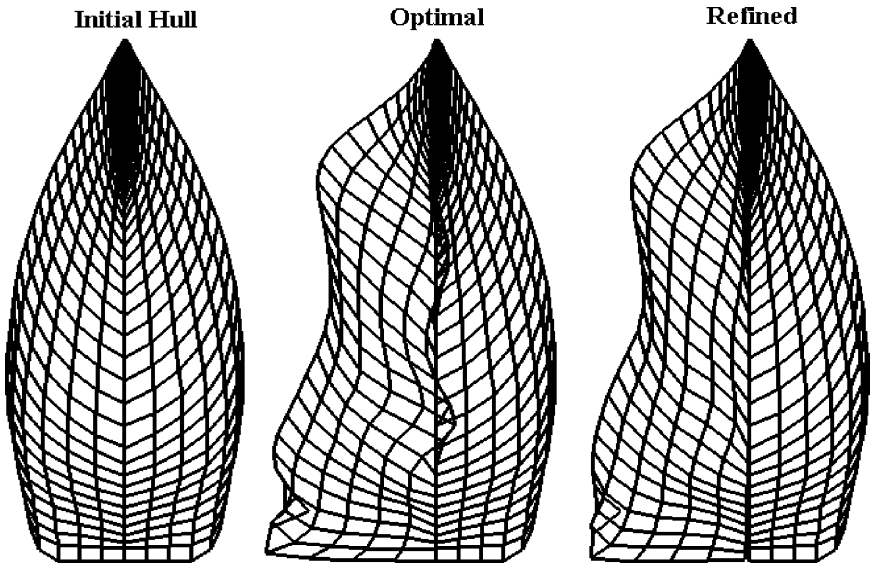

Fig. 9. Comparison of panelized hull forms for initial, optimal, and refined hulls with $\omega = 0.1$ in Section 6.2.

A comparison of panelized hull form with $\omega = 0.1$ is illustrated in Fig. 9, while body plans for an optimal hull predicted by the inverse design method with $\omega = 0.01$ and 0.1 are shown in Fig. 10(a) and (b), respectively. For $\omega = 0.01$, the optimal hull has an extreme V-shape frame with a semi-swath type transom stern. It is also noted that the bottom of this optimal hull crosses the ship center line. In this way, the blockage of the hull in shallow water can be alleviated. In other words, the optimal hull tends to reduce the ship draft and increase the clearance from the keel to the sea bottom. By moving the control points of the optimal hull at this region slightly outward to avoid the portside hull across the ship centerline, a refined hull can be obtained. The body plan of this refined hull is also plotted in Fig. 10(a) for comparison.

For $\omega = 0.1$, the resulting wave profile, panelized hull form and body plans are shown in Figs. 8, 9 and 10(b), respectively. Compare each body plan in Fig. 10, we find the ship is getting full when the weight coefficient increases. Meanwhile, the transom is changed from the semi-swath shape to wide trapezoid transom. In the same way, by comparing each wave profile in Fig. 8, it is noted that the wave profile is more deviated from the target wave as the weight coefficient increases. From Fig. 9, the optimal hull with $\omega = 0.1$ shows a longitudinal wavy tendency that forms a relatively hollow shape around the mid-ship area. Such a hull form will generate a relatively high dynamic pressure than the plump mid-ship such that the amplitude of wave trough can be reduced. From the pressure contour plot of Cp on the free surface in Fig. 11(a), it is revealed that the wave is reduced significantly.

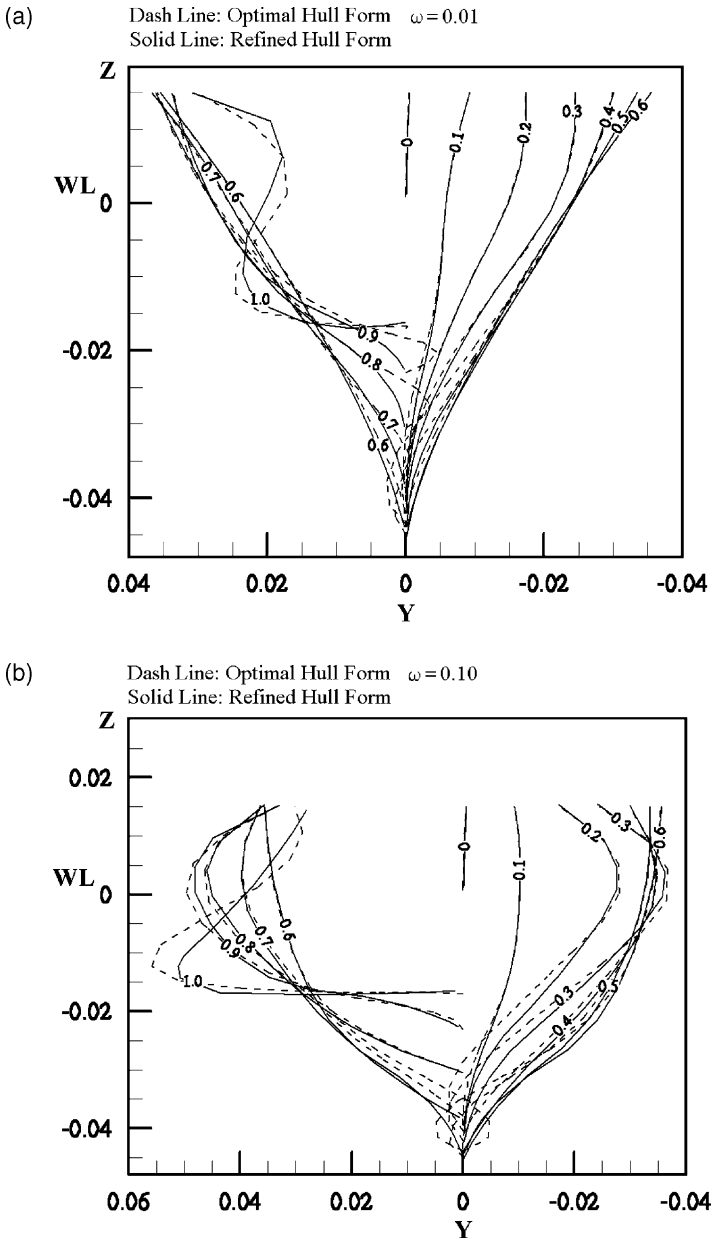

Fig. 10. Body plans for the optimal and refined hulls with (a) $\omega = 0.01$ and (b) $\omega = 0.10$.

The numerical results for the initial and optimal hulls with $\omega = 0.01$, 0.05 and 0.1 are summarized in Table 2.

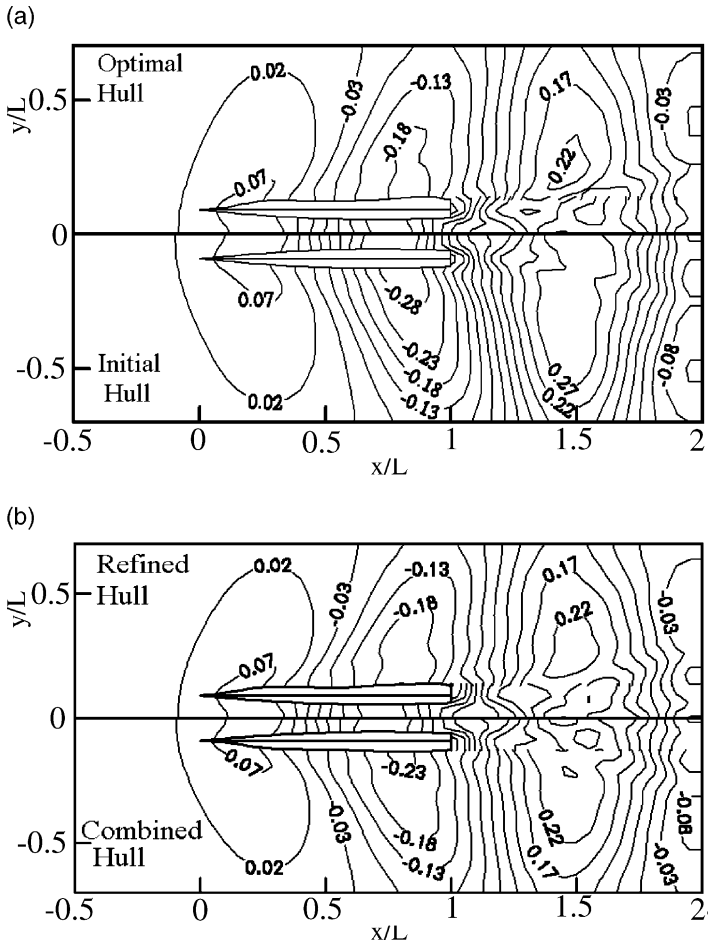

Fig. 11. Cp plots of free surface for (a). initial and optimal hulls with $\omega = 0.1$ and (b) refined and combined hulls with $\omega = 0.1$.

Table 2
The numerical results of inverse hull design in Section 6.2

Conventional (initial ship)	catamaran $\omega = 0.01$	$\omega = 0.05$	$\omega = 0.10$	$\omega = 0.01$ (Refined hull)	$\omega = 0.10$ (Refined hull)
Cw_linear	100.00%	55.90%	51.33%	56.63%	57.75%	70.85%
Volume	100.00%	73.74%	86.60%	97.93%	75.67%	100.57%
σ_h	–	5.30E-05	1.21E-04	1.07E-04	7.94E-05	1.81E-04
CPU (s)	102	12,243	7,064	9,923	103	101
Iteration	–	5	3	4	–	–

As mentioned above, some bottom regions of these optimal hulls predicted by the inverse method tend to cross the ship centerline. To rectify this, a refined hull is generated by moving the relevant control points outward. From Table 2, we note that the wave resistance of the refined hull is quite close to that of the optimal hull for $\omega = 0.01$ case. However, for the $\omega = 0.01$ case, the wave resistance is significantly increased from the optimal hull to the refined hull. We had tried several times to make a better refined hull but did not succeed and the Cw value of all refined hulls is still in the similar level. Therefore, we infer that for the slightly full form catamaran such as $\omega = 0.1$ case, the wash wave of critical speed is sensitive to the clearance between the keel and sea bottom.

To summarize the inverse design approach for the catamaran with minimizing ship wave at the critical speed in shallow water, the optimal hull turns out to be the V-shape frames if the requirement of displacement is looseness. When increasing the demand for the displacement constraint, the optimal hull exhibits a longitudinal wavy tendency which will cancel the wash wave by hull wave interaction, at the same time, the transom also becomes a wide trapezoid shape. The optimal hull tends to eliminate the displacement in the bottom region. All of these features appeared in the Leer-Andersen and Larsson (1999) paper. The proper Lagrangian multiplier for the equality constraint on volume of the estimated hull is the value $\omega = 0.1$, which is one-fifth weighted in the objective function of Eq. (7).

6.3. *Minimizing wash wave in deep water*

To illustrate how to minimize the ship wave in deep water conditions by the inverse method, two different target wave heights are surveyed in this section. The first target wave resulted from the wave profile of the initial hull by setting the bow wave as 0.85 times and the wave trough and the downstream wave as 0.75 times of the initial hull. The second target wave is obtained by reducing the wave trough and the downstream wave to a further low value of 0.70 times. To maintain the displacement in the same level of initial hull, the Lagrangian multiplier for volume constraint is set as $\omega = 0.1$ in the target function. To obtain a convergent estimation, the stopping criteria of inverse computation is loosened appropriately to the value of $\varepsilon = 6.7 \times 10^{-5}$.

After performing the calculation of inverse design, two optimal hulls, Opt_A and Opt_B, corresponding to the first and second target waves are obtained, respectively. The wave profiles for the initial, target, optimal and refined hulls are shown in Fig. 12. From Fig. 12, we note that the amplitude of wave for the optimal hulls is larger than that for the target wave. This infers that there is no hull form with the specified target displacement within the freedom granted in the hull generation process can produce such small wave. Thus it is futile to pursue a further reduced wave height as the design target.

The body plans for Opt_A, Ref_A (i.e. the refined hull for Opt_A) and Opt_B, Ref_B (i.e. the refined hull for Opt_B) are shown in Fig. 13(a) and (b), respectively. The panelized hull forms for the Ref_A and Ref_B are plotted in Fig. 14. The key feature of these optimal hulls is that there is a bulbous bow appearing on the bow

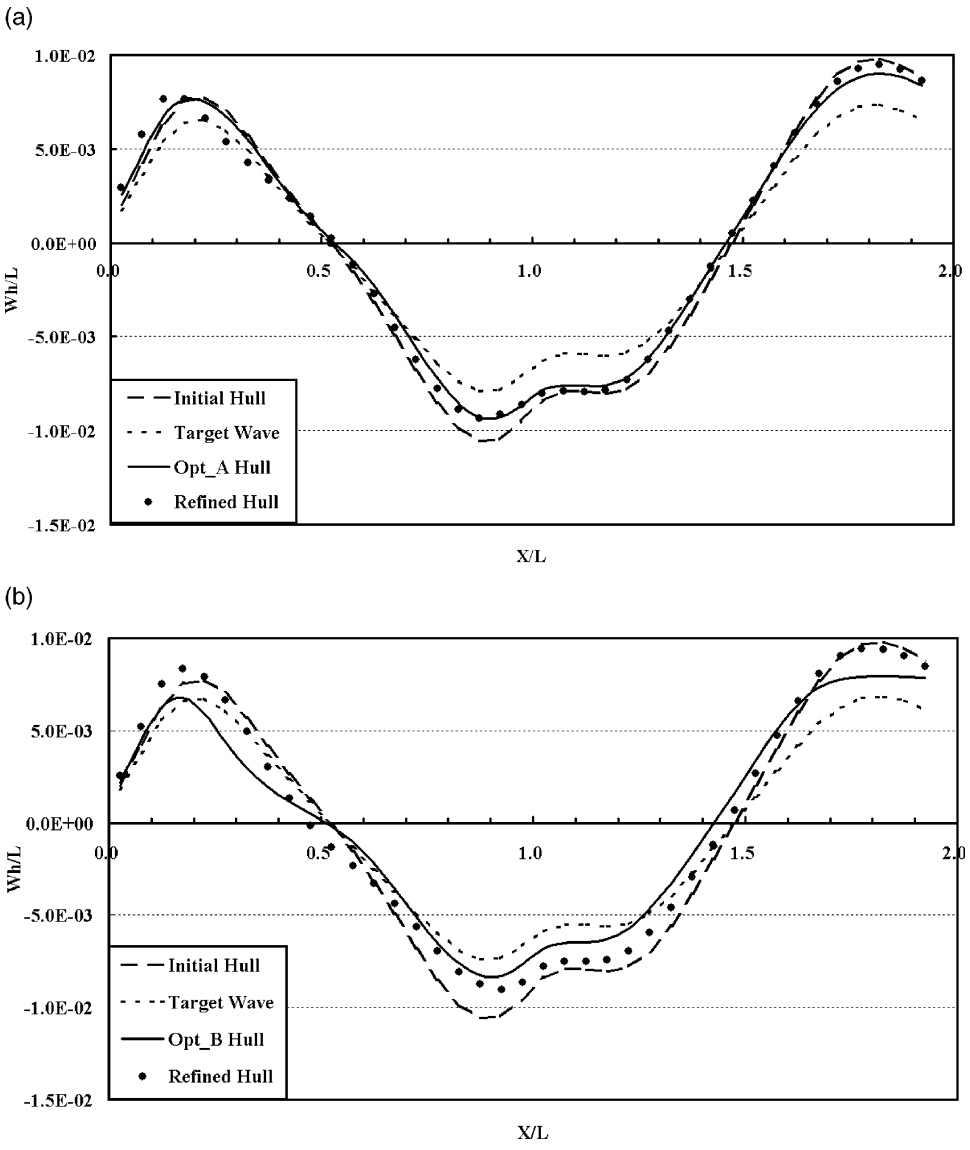

Fig. 12. Comparison of wave profile along catamaran's outside for (a) the initial, Opt_A and refined hulls and (b) the initial, Opt_B and refined hulls.

region and the entrance angle becomes very small. The latter yields the waterline entrance of the portside ship twisting across the ship centerline. This enlightens us that the small entrance angle together with the bulbous bow is a key feature for the ship with reduced wave at this design condition. In addition to the narrowed waterline entrance, some frame line around the keel area of the optimal hull is

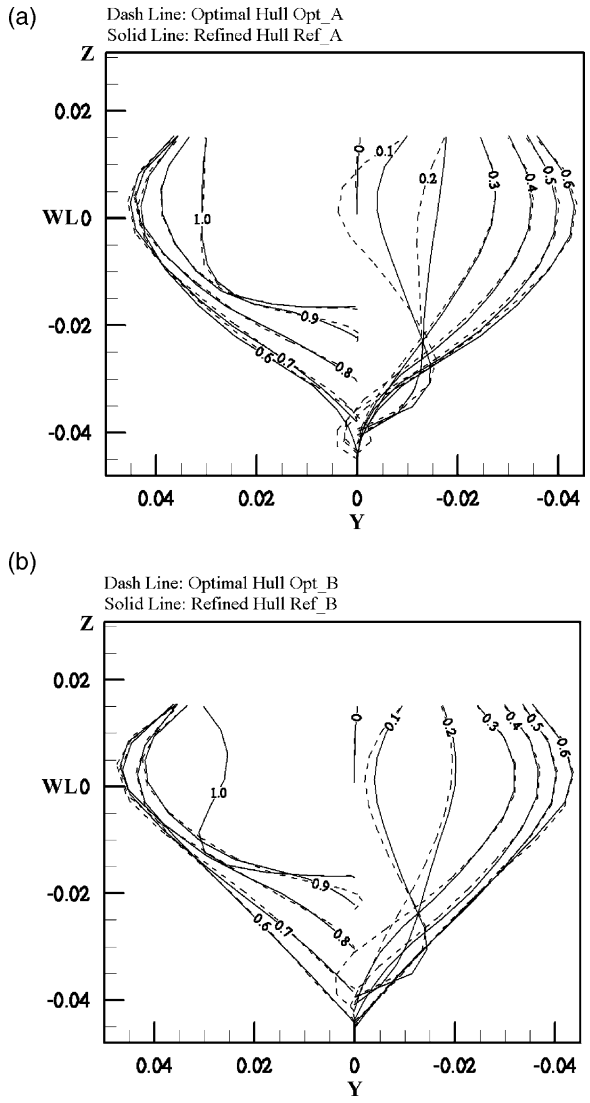

Fig. 13. Body plans for (a) Opt_A and Ref_A and for (b) Opt_B and Ref_B.

slightly prone to cross the ship centerline. Both features are adverse to ship production. To rectify these, we proceed to refine the hull by moving the dominated control points outward.

Compare the body plans of Opt_A with Opt_B in Fig. 13, one can find that the frame line of Opt_A hull is the bulging V shape and Opt_B is the straight V shape. In addition, both Opt_A and Opt_B hulls are a monotonic curve that is different from the longitudinal wavy tendency for the optimal hull in shallow water.

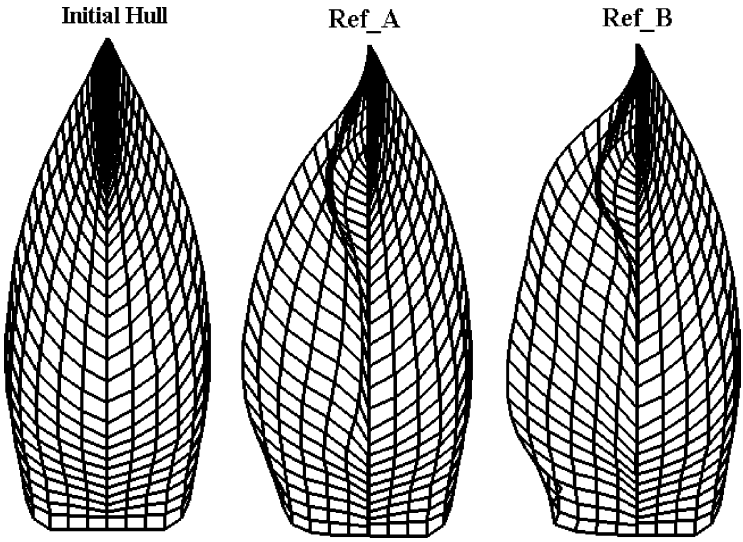

Fig. 14. Comparison of panelized hull form of Section 6.3 for the Initial, Ref_ A, and Ref_B hulls.

Although the full breadth of the optimal hull is wider than the initial hull, both transom of Opt_A and Opt_B are kept in the same level as the initial hull. The transom stern of Opt_A hull is the same as the initial hull but the transom stern of Opt_B hull tends to reduce the waterplane area. This feature helps the Opt_B hull to generate smaller wave trough to close the severer target wave.

The Cp contour of the free surface for the initial, optimal and refined hulls are illustrated in Fig. 15. The numerical results for the initial, optimal and refined hulls subject to different target waves are summarized in Table 3. From these Cp plots, one can see that the wave trough of optimal hull is reduced significantly when compared with the initial hull. However, the improvements at wave trough of the refined hulls are slightly worse than the optimal hulls, especially, from Opt_B hull to Ref_B hull. This probably means that the modified parts from Opt_B to Ref_B are very critical. The deviation also reflects the Cw value and the σ_h in Table 3. Regarding that both refined hulls are in the same level, we suppose that even a severer target wave is utilized such as Opt_B case, the actual hull form may lose the superiority during the refinement process. Thus, it is not necessary to try a smaller target wave or the demand for the equality of displacement volume should be loosened.

To summarize the applying of inverse design schemes to minimize the ship wave, we recommend the ship designer trial a tighter target wave by modifying the value of the parent ship, and then carefully refine the hull or reset a new target wave refer to the results of first trial. By applying the inverse design scheme, the optimal hull design problem for the minimizing ship wave is simplified to design the proper target wave.

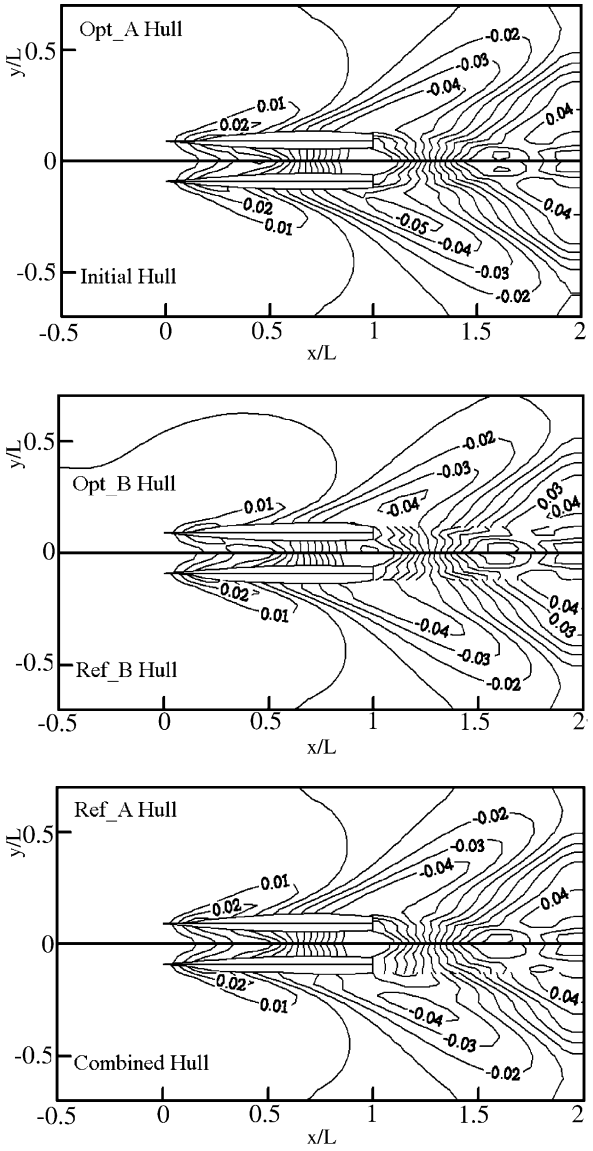

Fig. 15. Cp plot of free surface (deep-water case $Fn_L = 0.6428$) for the initial, optimal, refined and the combined hulls.

6.4. Optimal hull for deep water and shallow water

In general, the focus of the design of an ordinary ship is on one design condition and the ship operator will try to avoid running the ship in critical conditions for a long period. However, to explore the possible results for a hull performing well in

Table 3
The numerical results of inverse hull design in Section 6.3

Conventional catamaran (initial ship)		Opt_A	Opt_B	Ref_A	Ref_B
Cw_linear	100.00%	82.99%	77.17%	86.55%	88.95%
Cw_nonlinear	100.00%	89.31%	79.49%	93.89%	94.88%
Volume	100.00%	95.71%	97.18%	98.11%	99.68%
σ_h	–	4.80E-05	5.28E-05	7.04E-05	9.87E-05
CPU (s)	68	6,180	6,148	64	64
Iteration	–	4	4	–	–

both conditions, we simply average the control points of both optimal hulls for deep water and shallow water to create a combined hull. This way may not generate the optimal hull but at least it provides the combining feature of both optimal hull forms. The combined hull is the combination of Ref_A and the refined optimal hull of shallow water with $\omega = 0.1$. The body plan and panelized hull form for the combined hull are plotted in Fig. 16(a) and (b), respectively. In Fig. 16 one can note that both features of each optimal hull at different water depths such as bulbous bow, small entrance angle, slightly longitudinal wavy form and wide flat transom stern appear in the combined hull.

The wave profiles for the combined hull and refined optimal hulls at different water depth and different ship speed are plotted in Fig. 17. At the critical speed of shallow water, the wave profile of the combined hull is quite close to the refined optimal hull in shallow water. By contrast, the combined hull in deep-water con-

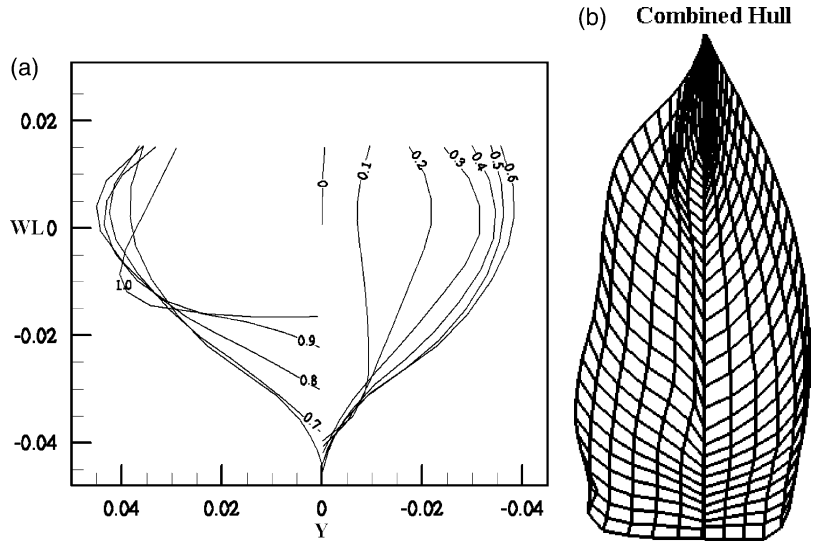

Fig. 16. (a) Body plan and (b) panelized hull form for the combined hull form.

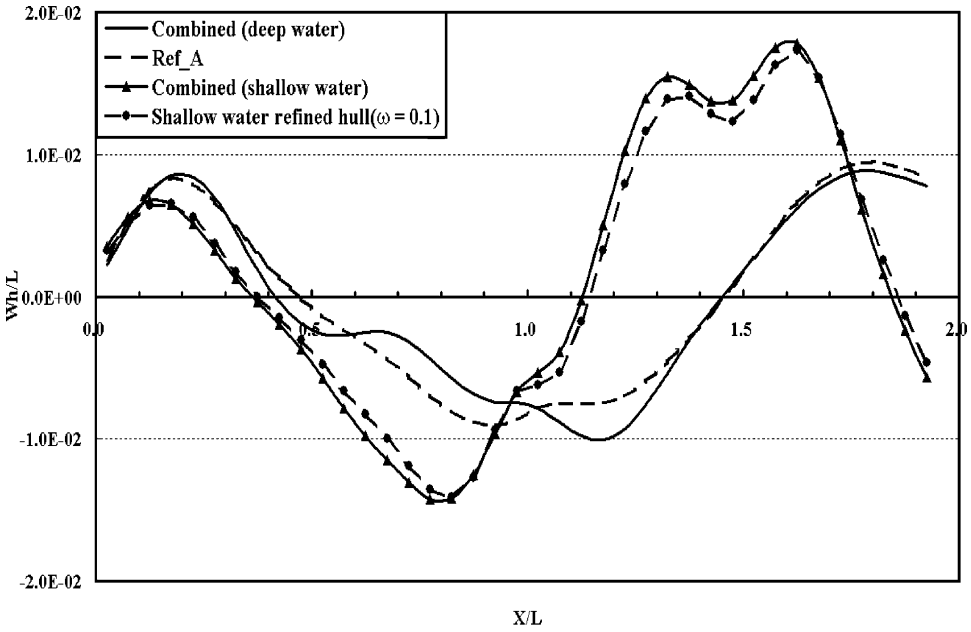

Fig. 17. Comparison of wave profile for the combined hull and the refined optimal hulls at shallow water and deep water.

ditions generates wavier wave profile than the Ref_A hull. This is due to its slightly longitudinal wavy form. Despite the deviation of the wave profile in deep-water conditions, the combined hull still generates a small ship wave which can be found by comparison of the pressure contour on the free surface in Fig. 15. The pressure contour of the free surface as shown in Fig. 11(b) also indicates that the ship wave of the combined hull is also good in the critical speed of shallow water.

The numerical results at two water depths and speeds for the initial, semi-swath, and the combined hulls are summarized in Table 4. The improvement of this combined hull at critical speed is more obvious than the results in deep water. In addition, the tendency of the nonlinear free surface solution is similar to the linear solution but the improvement level is not so significant. Compare Table 4

Table 4
The numerical results of combined hull form in Section 6.4

	Deep water $Fn_L = 0.6428$			Shallow water $Fn_d = 1.0$		
	Conventional catamaran	Semi-swath	Combined hull	Conventional catamaran	Semi-swath	Combined hull
Cw_linear	100.00%	90.91%	85.28%	100.00%	94.49%	71.95%
Cw_nonlinear	100.00%	90.02%	94.18%	100.00%	86.80%	84.31%
Volume	100.00%	91.96%	98.82%	100.00%	91.96%	98.82%

with Tables 2 and 3, we confirm that the wave resistance of the combined hull is as good as each optimal hull in different water depth conditions and is better than the initial hull (i.e. conventional catamaran).

7. Conclusions

An inverse design problem in estimating the optimal hull form of minimizing wave from the desired wave distribution by the techniques of B-spline surface fitting and Levenberg–Marquardt method has been developed and applied successfully.

To improve the accuracy of the inverse hull prediction, the constraint on displacement volume is, for the first time, included in the objective functional. Results show that the present algorithm needs only a few iterations to obtain the optimal hull. The required CPU for each optimal hull on an SGI Octane machine is very limited to only about two to three hours.

The optimal hull of minimum wave at the critical speed in shallow water tends to eliminate the displacement in the bottom region so that it leads to the V-shape frames. In addition, the optimal hull exhibits a longitudinal wavy tendency, which will cancel the ship wave by the hull wave interaction, and the transom becomes a wide trapezoid shape. The optimal hull of minimizing wave at the studied condition in deep-water has the feature of the monotonic V-shape frames with the bulbous bow and small entrance angle. A combined hull with features of both optimal hulls fortunately also performs well in both water depth and speed.

Regarding that the ship wave is the source of wash wave to coast, the hull form designed by the present scheme can be friendly to the coast environment and also reduce the operation cost (i.e. energy saving). The application of the present algorithm is not only limited to the catamaran but also applicable to general vessels like the container vessel, ferries or further, fishing vessels in the lagoon.

Acknowledgements

This work was supported in part through the National Science Council, R.O.C., Grant number, NSC-90-2611-E-006-022 and NCKU-NSYSU research center of Ocean Environmental and Engineering Technology.

References

Day, A.H., Doctors, L.J., 2001. Concept evaluation for high-speed low-wash vessels. Proceeding: FAST 2001. Southampton, UK.

Chen, P.F., Huang, C.H., 2002. An inverse hull design problem in optimizing the desired wake of ship. Journal of Ship Research 46, 138–147.

Huang, C.H., Huang, M.C., 1994. Inverse problem in determining the normal and tangential drag coefficients of marine cables. Journal of Ship Research 38, 296–301.

Huang, C.H., Ozisik, M.N., 1991. A direct integration approach for simultaneously estimating temperature dependent thermal conductivity and heat capacity. Numerical Heat Transfer, Part A 20, 95–110.

Huang, C.H., Wang, D.M., 1996. Statistical consideration for the estimation of spatially varying sound velocity and water density in acoustic inversion. Inverse Problems in Engineering 4, 129–151.

Huang, C.H., Chiang, C.C., Chou, S.K., 1998. An inverse geometry design problem in optimizing hull surfaces. Journal of Ship Research 42, 79–85.

Larsson, L., Broberg, L., Kim, K.J., Zhang, D.H., 1989. New viscous and inviscid CFD techniques for ship flows. Proceedings: 5th International Conference on Numerical Ship Hydrodynamics, The National Academic Press, Hiroshima, Japan.

Larsson, L., Kim, K.J., Esping, B., Holm, D., 1992. Hydrodynamic optimization using SHIPFLOW. Proceedings: 5th International Symposium on Practical Design of Ships and Mobile Units. Newcastle upon Tyne, UK, 1, 1.1–1.16.

Larsson, L., 1999. SHIPFLOW User's Manual. FLOWTECH International AB, Gothenburg, Sweden.

Leer-Andersen, M., and Larsson, L., 1999. Non-interactive optimisation of hull shapes with regards to minimizing wash waves. Proceeding: HIPER'99, Zevenwacht, South Africa.

Lin, W.C., Webster, W.C., Wehausen, J.V., 1963. Ship of minimum total resistance. In: Proceedings: International Seminar on Theoretical Wave-Resistance, The University of Michigan, Ann Arbor, pp. 907–953.

Lowe, T.W., Bloor, M.I.G., Wilson, M.J., 1994. The automatic functional design of hull surface geometry. Journal of Ship Research 38, 319–328.

Marquardt, D.M., 1963. An algorithm for least-squares estimation of nonlinear parameters. J. Soc. Indust. Appl. Math. 11, 431–441.

Wood, W.A., 2000. High-speed ferry issues for operators and designers. Marine Technology 37, 230–237.

Wyatt, D.C., Chang, P.A. 1990. Development and assessment of a total resistance optimized bow for the AE-36. Proceedings: The International Symposium on CFD and CAD in Ship Design. Elsevier Science Ltd., Wageningen, The Netherlands.

Yang, C., Soto, O., Lohner, R., 2002. Hydrodynamic optimization of a trimaran. Ship Technology Research 49, 70–92.

Yang, Q., Faltinsen, O.M., Zhao, R., 2001. Wash of ships in finite water depth. Proceeding: FAST 2001, The Royal Institution of Naval Architects, Southampton, UK.